

## Article

## Mechanisms of Gold Bioaccumulation by Filamentous Cyanobacteria from Gold(III)–Chloride Complex

Maggy F. Lengke, Bruce Ravel, Michael E. Fleet, Gregory Wanger, Robert A. Gordon, and Gordon Southam

*Environ. Sci. Technol.*, **2006**, 40 (20), 6304-6309 • DOI: 10.1021/es061040r • Publication Date (Web): 09 September 2006

Downloaded from <http://pubs.acs.org> on April 13, 2009

### More About This Article

Additional resources and features associated with this article are available within the HTML version:

- Supporting Information
- Links to the 3 articles that cite this article, as of the time of this article download
- Access to high resolution figures
- Links to articles and content related to this article
- Copyright permission to reproduce figures and/or text from this article

[View the Full Text HTML](#)



**ACS Publications**  
High quality. High impact.

# Mechanisms of Gold Bioaccumulation by Filamentous Cyanobacteria from Gold(III)–Chloride Complex

MAGGY F. LENGKE,<sup>\*,†</sup> BRUCE RAVEL,<sup>‡</sup> MICHAEL E. FLEET,<sup>†</sup> GREGORY WANGER,<sup>†</sup> ROBERT A. GORDON,<sup>§</sup> AND GORDON SOUTHAM<sup>†</sup>

Department of Earth Sciences, University of Western Ontario, London, Ontario N6A 5B7, Canada, Argonne National Laboratory, Argonne, Illinois 60439, and Simon Fraser University, Burnaby, British Columbia V5A 1S6, Canada

The mechanisms of gold bioaccumulation by cyanobacteria (*Plectonema boryanum* UTEX 485) from gold(III)–chloride solutions have been studied at three gold concentrations (0.8, 1.7, and 7.6 mM) at 25 °C, using both fixed-time laboratory and real-time synchrotron radiation absorption spectroscopy (XAS) experiments. Interaction of cyanobacteria with aqueous gold(III)–chloride initially promoted the precipitation of nanoparticles of amorphous gold(I)–sulfide at the cell walls, and finally deposited metallic gold in the form of octahedral (111) platelets (~10 nm to 6 μm) near cell surfaces and in solutions. The XAS results confirm that the reduction mechanism of gold(III)–chloride to metallic gold by cyanobacteria involves the formation of an intermediate Au(I) species, gold(I)–sulfide.

## Introduction

Gold is one of the rarest metals on earth, and its importance has been known since antiquity. Because of the increased demand for gold in industry and nanotechnology, exploration for new gold deposits in the natural environment has become very important. On the other hand, gold in waste solutions from several industrial processes, e.g., gold mining and gold electroplating effluents, could be recovered and reused. Therefore, there is an essential need to develop alternative cost-effective and environmentally sound methods for recovering gold from waste solutions.

The deposition of gold in primary deposits usually occurs via metal-rich hydrothermal fluids, which circulate in open spaces within rocks and deposit gold as a consequence of cooling or boiling, forming lode and disseminated gold deposits (1). In lode deposits, gold particles are contained in quartz veins within country rocks, whereas in disseminated gold deposits, gold mineralization is evenly distributed throughout the deposit and not concentrated in veins. The weathering of primary gold-bearing deposits mobilizes gold as complexes with chloride ( $\text{AuCl}_4^-$ ) and/or thiosulfate ( $\text{Au}(\text{S}_2\text{O}_3)_2^{3-}$ ) in surface or near-surface environments (2–4). The interaction of these gold complexes with the biosphere

(e.g., microorganisms) results in the deposition of secondary gold, forming placer and reef-type deposits. Placer deposits are composed of unconsolidated materials such as gravel and sands in which gold particles occur as free particles. In reef-type deposits, gold exists in quartz conglomerates, and these deposits generally result from consolidation of placer deposits. The world's gold production has mostly come from mining reef-type and placer deposits. The deposition of secondary gold in the natural environment from localities in Australia, Venezuela, Alaska, and South Africa has been attributed to bacteria and cyanobacteria (5–10). A number of laboratory experiments have been conducted to understand the interaction of gold with bacteria (e.g., *Bacillus subtilis*, *Escherichia coli* IAM 1264, *Pseudomonas maltophilia* IAM 1554) and cyanobacteria (e.g., *Plectonema terebrans*, *Plectonema boryanum* UTEX 485) using gold(III)–chloride ( $\text{AuCl}_4^-$ ) (11–18). Studies by Southam and Beveridge (12–13) demonstrated the formation of metallic gold with octahedral habit by organic phosphate and sulfur compounds derived from bacteria at pH ~2.6. Lengke et al. (18) observed similar octahedral metallic gold using *Plectonema boryanum* UTEX 485 at pH 1.9–2.2 and 25–200 °C. Fe(III)-reducing bacteria reduced gold(III)–chloride prior to or simultaneously with adsorption of gold onto the cell surfaces at pH 7.0, and the reactions involved the hydrogenase enzyme from these bacteria (14). The formation of gold by magnetotactic cocci was observed inside granules containing phosphorus, sulfur, and iron, and it was suggested that the sulfur-containing component of the granules is much more important in gold reduction than the phosphorus-containing component (17). Gold has also been observed within the cells of *Lactobacillus* sp., but the mechanisms of gold reduction were not discussed (21). The accumulation of gold by other bacteria (e.g., *Bacillus subtilis*, *Escherichia coli* IAM 1264, *Pseudomonas maltophilia* IAM 1554) at pH 1 to 6, and the precipitation of gold on the sheaths of *Plectonema terebrans* were hypothesized to take place through adsorption on the cells, although the precise mechanisms were poorly understood (11, 16).

A better understanding of the mechanisms of gold bioaccumulation by bacteria and cyanobacteria is required to improve our ability to detect anomalously rich gold deposits in the natural environment and to optimize gold recovery from aqueous solutions (19). Therefore, the goal of this study was to investigate the mechanisms of gold bioaccumulation using gold(III)–chloride ( $\text{AuCl}_4^-$ ) in the presence of cyanobacteria. The organism chosen for this study is the cyanobacterium *Plectonema boryanum* UTEX 485, because cyanobacteria form one of the largest and most important groups of bacteria on earth, are commonly found in natural environments, and are easily produced. This study was conducted using a combination of laboratory-based cyanobacterial experiments supported by transmission electron microscopy (TEM) at the University of Western Ontario (UWO), and real-time experiments by X-ray absorption spectroscopy (XAS) at the Advanced Photon Source, Argonne National Laboratory (Table 1). X-ray absorption near edge structure (XANES) provides information on the oxidation state of gold, and extended X-ray absorption fine structure (EXAFS) provides detailed information on the coordination environment about the absorbing atom, including the number and species of the neighboring atoms bound to the gold and the distances to those neighbors. Elucidation of the functional groups derived from the cyanobacteria for gold binding is required to understand chemical mechanisms of gold accumulation by cyanobacteria.

\* Corresponding author phone: (519) 661-2111, ext. 86109; fax: (519) 661-3198; e-mail: mlangke@uwo.ca or maggylengke@yahoo.com.

† University of Western Ontario.

‡ Argonne National Laboratory.

§ Simon Fraser University.

**TABLE 1. Gold Contents and Starting Proportions for the Cyanobacterial Experiments.**

initial Au [mM]	starting mixture <sup>a</sup>	total volume (mL)
<b>laboratory experiments</b>		
0.8	30 mL of 2.5 mM Au + 70 mL of Cyanobacteria	100
1.7	10 mL of 11.9 mM Au + 60 mL of Cyanobacteria	70
7.6	20 mL of 26.6 mM Au + 50 mL of Cyanobacteria	70
<b>XAS experiments</b>		
0.8	0.3 mL of 2.5 mM Au + 0.7 mL of Cyanobacteria	1
1.7	0.1 mL of 11.9 mM Au + 0.6 mL of Cyanobacteria	0.7
7.6	0.2 mL of 26.6 mM Au + 0.5 mL of Cyanobacteria	0.7

<sup>a</sup>Stock solutions contain ~20 mg/mL cyanobacteria (dry weight), and 15.8, 23.4, and 104.8 mg of Au in 0.8, 1.7, and 7.6 mM experiments, respectively.

## Materials and Methods

**Cyanobacteria Cultures.** The filamentous cyanobacterium, *Plectonema boryanum* UTEX 485 (obtained from the culture collection at the University of Texas at Austin, TX), was grown in batch cultures in BG-11 medium (20) and buffered with 10 mM HEPES at a control temperature of 29 °C under ambient CO<sub>2</sub> conditions. The pH of the medium was adjusted to 8.0 using 1 M NaOH solution. Before experimentation, the culture was transferred (20% [v/v] of inoculum) and grown 6–8 weeks to reach stationary “growth” phase. It was then centrifuged and washed three times with sterile, distilled, deionized water to remove salts and trace metals from the medium.

**Laboratory-Based Cyanobacterial Experiments.** The cyanobacterial experiments were conducted at the University of Western Ontario (UWO) to examine the role of cyanobacteria in the bioaccumulation of gold from aqueous solutions of gold(III)–chloride [HAuCl<sub>4</sub>·3H<sub>2</sub>O; Alfa Aesar Company, Ward Hill, MA]. To initiate the experiments, gold solutions (with 0.8, 1.7, and 7.6 mM initial dissolved gold; Table 1) were added to a washed cyanobacteria culture (~20 mg/mL dry weight). The experiments were conducted at 25 °C for 24 h. pH, *E<sub>h</sub>*, total gold, phosphorus, and sulfur, and cyanobacteria populations were measured with time. All experiments were conducted in duplicate.

**Bacterial Viability and Total Bacterial Counts.** The effects of gold(III)–chloride solutions on the cyanobacteria were monitored during the course of the cyanobacterial experiments by determining bacterial viability using the LIVE/DEAD BacLight bacterial viability kit (L-7007, Molecular Probes, Inc., Eugene, OR). When viewed with a fluorescence microscope, viable bacteria stained with the LIVE/DEAD BacLight reagents appear green, whereas dead bacteria appear red. The total number of bacteria in the cultures was determined by the direct counting method using a Petroff–Hauser counting chamber and a phase contrast light microscope (Nikon Labophot microscope).

**Chemical Analyses.** The pH and *E<sub>h</sub>* were monitored using a Denver Instrument Basic pH/ORP/temperature-meter. The pH electrode was calibrated using buffer solutions 4, 7, and 10 with analytical uncertainties in pH measurements of ± 0.05 pH unit. The *E<sub>h</sub>* was measured using an ORP electrode and calibrated using ZoBell’s solution (21).

Total gold, sulfur, and phosphorus concentrations were measured over the course of the experiments with a Perkin-Elmer 3300-DV inductively coupled plasma optical emission spectrometer (ICP-OES). The uncertainty in measured gold,

sulfur, and phosphorus is ≤5%, with detection limits of 0.25 μM, 0.03 mM, and 0.02 mM for gold, sulfur, and phosphorus, respectively.

Procedures for TEM and XAS are described in the Supporting Information.

## Results and Discussion

**Cyanobacterial Experiments.** On the addition of gold(III)–chloride to the cyanobacteria culture, total gold concentrations decreased significantly at all three gold concentrations (0.8, 1.7, and 7.6 mM), as shown in the Supporting Information (Figure S1). Total soluble sulfur and phosphorus concentrations increased significantly within several minutes of the reactions and remained relatively constant until the completion of the experiments for 0.8 and 1.7 mM initial gold, but for 7.6 mM initial gold the sulfur and phosphorus concentrations increased gradually with time (Supporting Information, Figure S1). The cyanobacteria were killed several minutes after the addition of gold(III)–chloride.

At 0.8 mM initial gold, the pH and *E<sub>h</sub>* values were relatively constant at ~3 and ~0.73 V, respectively. The color of the cyanobacteria remained green, but dark purple color was observed in the solution after several hours of reaction. The purple color in the solution is characteristic of formation of colloidal gold.

At 1.7 mM initial gold, on addition of gold(III)–chloride to the cyanobacteria, change was observed in the color of the cyanobacteria and solutions, from green to reddish brown and yellow to colorless, respectively. The pH and *E<sub>h</sub>* values were relatively constant at ~2.2 and ~1.05 V, respectively.

At 7.6 mM initial gold, the soluble gold concentration decreased with increase in reaction time by about 7 mM. Total soluble sulfur and phosphorus concentrations increased gradually from 0.00 to ~0.55 mM and to ~0.20 mM, respectively, during the course of experiments. The pH and *E<sub>h</sub>* values were relatively constant at ~1.9 and ~1.11 V, respectively.

The aqueous gold(III)–chloride solutions at all gold concentrations investigated were stable for one week in abiotic experiments (without the presence of cyanobacteria) under similar conditions.

**TEM.** On the addition of gold(III)–chloride to the cyanobacteria, precipitation of nanoparticles (<20 nm) containing gold, sulfur, phosphorus, carbon, and nitrogen was observed by TEM-EDS at the cell surfaces and at the interface between the cell wall and solution within several minutes (Figure 1A). These nanoparticles were amorphous to electron diffraction. The TEM-EDS for the cyanobacterial samples after 2 h reaction time also showed the association of gold with sulfur, phosphorus, and nitrogen in the cyanobacteria cells and at the cell walls (Supporting Information, Figure S2). This suggests that sulfur and gold were involved in the formation of nanoparticles, and nitrogen from cell material is indirectly related to the gold binding process. After 17 h, the dead cyanobacteria released cytoplasmic material around the cells, causing further precipitation of metallic gold nanoparticles (Figure 1B), with octahedral and sub-octahedral shapes and diameters up to 6 nm (Figure 1C and E). TEM-SAED of these angular nanoparticles revealed powder ring diffraction patterns (Figure 1D) consistent with nanocrystalline gold, and the presence of metallic gold with octahedral (111) crystal faces (Figure 1F). A tendency for the frequency of larger octahedral platelets to increase with run duration indicated a weak Ostwald ripening effect.

**XAS.** *XANES Spectra of Model Compounds.* The XANES spectra of the model compounds including gold(III)–chloride, gold(III)–hydroxide, gold(III)–thiocyanate, gold(I)–chloride, gold(I)–cyanide, gold(I)–thiosulfate, gold(I)–sulfide, gold(I)–thiomalate, gold(I)–chloro(triphenylphosphine), and gold foil are shown in the Supporting Information (Figure S3). Typical Au-L<sub>3</sub> edge XANES spectra are shown in

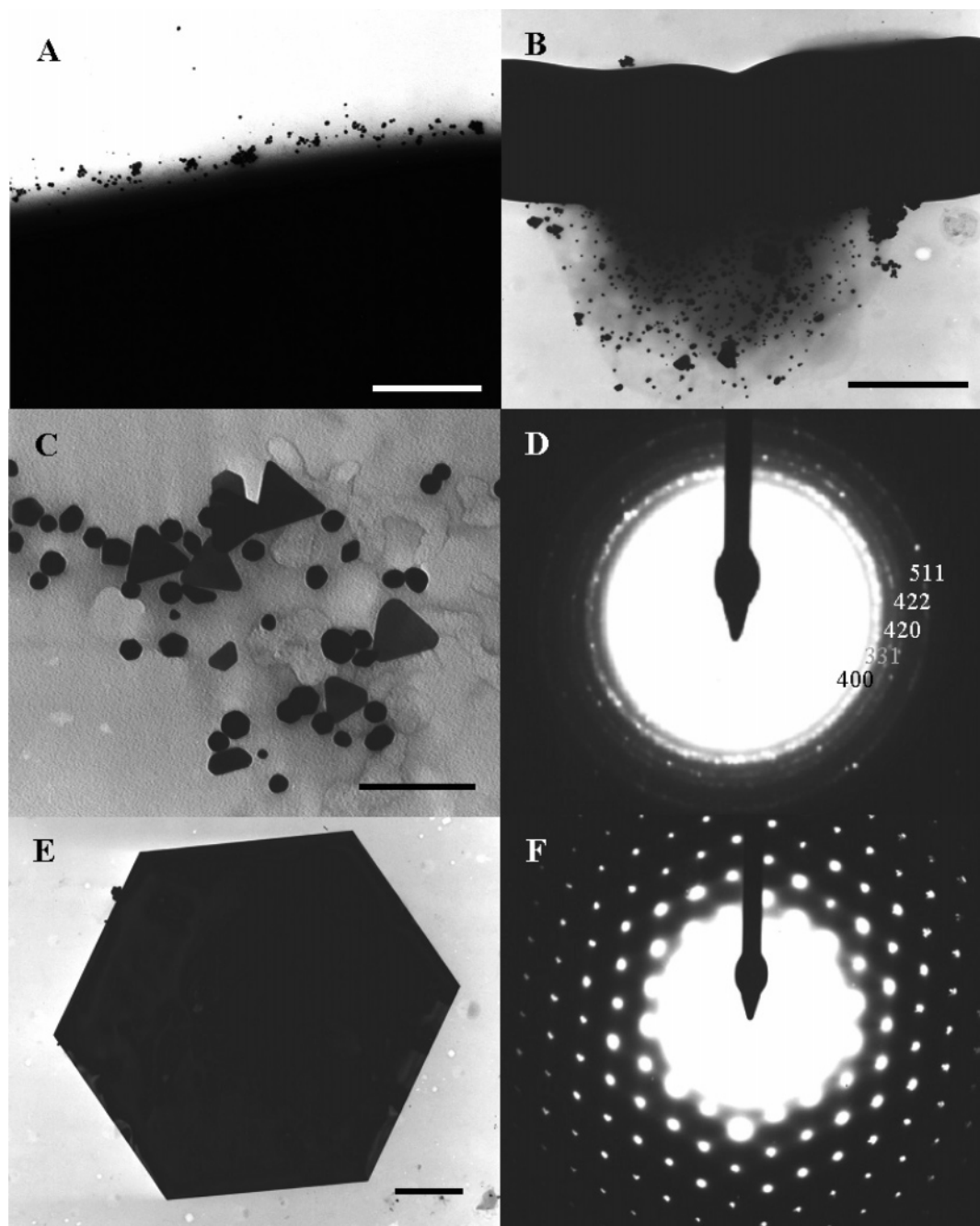


**FIGURE 1.** TEM micrographs of whole mounts of cyanobacterial cells cultured in the presence of gold(III)–chloride and nanoparticles of gold with corresponding TEM-SAED diffraction pattern at 25 °C at UWO: (A) precipitation of nanoparticles at cell boundary at 10 min for 1.7 mM initial gold; (B) precipitation of nanoparticles of gold associated with the cell material at 17 h for 1.7 mM initial gold; (C, D) at 0.8 mM initial gold and 17 h; (D) TEM-SAED diffraction powder-ring pattern consistent with crystalline nanoparticles of Au; *d*-spacings of 0.102, 0.094, 0.0912, 0.0832, and 0.0785 nm correspond to reflections 400, 331, 420, 422, and 511, respectively; other lines visible on the SAED negative with *d*-spacings of 0.144, 0.123, and 0.118 nm correspond to reflections 220, 311, and 222; (E, F) at 7.6 mM initial gold and 17 h; (F) TEM-SAED twinned diffraction pattern consistent with crystalline gold. Scale bars in A, B, C, and E are 0.3, 0.75, 0.1, and 1  $\mu\text{m}$ , respectively.

Figures 2 and 3. The absorption edge of gold(III) and gold(I) compounds shifts to lower energy compared to the gold foil. This unusual edge shift for Au(III) is readily attributed to the low-energy dipole-allowed 2p to 5d transition, which is allowed for the  $d^8$  species and forbidden for  $d^{10}$  Au(0) (22). Oxidation states of gold are determined from the position and appearance of the intense and sharp Au-L<sub>3</sub> edge feature (23). The white line feature appears at approximately 11921 eV for Au(III) (e.g., gold(III)–chloride and gold(III)–hydroxide), but it shifts to higher photon energy with decreasing oxidation state of gold, as presented in Figures 3 and S3. For gold foil, the XANES postedge peak at approximately

11947 eV is characteristic of Au(0) (Figures 3 and S3). Therefore, the white line feature and its intensity were used for the determination of oxidation state of gold. The Au-L<sub>3</sub> XANES spectra for the solutions of the selected model compounds (gold(III)–chloride, gold(I)–thiosulfate, and gold(I)–thiomalate) show spectra similar to those of the solids, confirming that the Au atoms remain complexed in aqueous solution (Supporting Information, Figures S3 and S4). We observed no changes in energy shifts of the edge position for measurements in solutions compared to corresponding solids. However, the spectrum of gold(I)–chloride in solution is not similar to the solid, indicating that gold(I)–



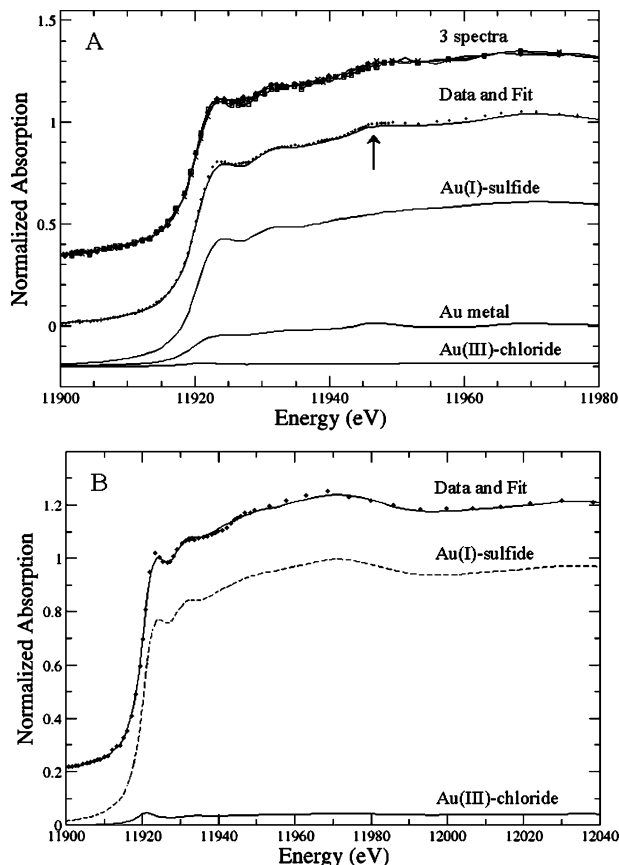


**FIGURE 2.** (A) XANES Au-L<sub>3</sub> edge spectra and LC-XANES fits for the cyanobacterial samples at 0.8 mM initial gold. The three spectra at the top are representative scans from the beginning, middle, and end of the sequence of scans as described in the text. (B) XANES Au-L<sub>3</sub> edge spectra and LC-XANES fits for the cyanobacterial samples at 1.7 mM initial gold. The weighted components are displayed below the fit.

chloride is unstable in solution (Supporting Information, Figure S4). At 25 °C and high concentration, gold(I)–chloride disproportionates to a mixture of gold(III)–chloride and gold metal (24), via the following reaction:



**XANES Spectra of Cyanobacterial Samples.** The *in situ*, real-time experiments were conducted on cyanobacterial samples at 0.8 and 1.7 mM initial gold for approximately 14 h, while the cyanobacterial experiments at 7.6 mM initial gold were conducted for approximately 40 h. At 0.8 mM initial gold, changes in spectra collected during the course of experiments were not observed. The Au-L<sub>3</sub> edge energy of the cyanobacterial sample at 0.8 mM initial gold showed a weak white line feature at approximately 11923 eV (Figure 2A). This feature showed that the majority of gold atoms were present as Au(I) (gold(I)–sulfide,  $78 \pm 2\%$ ) with Au(0) (gold metal,  $20 \pm 2\%$ ) and trace of Au(III) (gold(III)–chloride,  $2 \pm 1\%$ ). The XANES feature at approximately 11947 eV is characteristic of Au(0), showing that Au(0) was present in the sample (Figure 2A, indicated by an arrow).

At 1.7 mM initial gold, the spectra collected during the course of experiments showed very little change from the first to the last scans. The Au-L<sub>3</sub> edge energy of the cyanobacterial sample showed a less intense white line feature at approximately 11923 eV (Figure 2B). This feature showed that the majority of gold atoms were present as Au(I) (gold(I)–sulfide,  $96 \pm 1\%$ ) with trace of Au(III) (gold(III)–chloride,  $4 \pm 1\%$ ). The absence of the XANES peaks at approximately

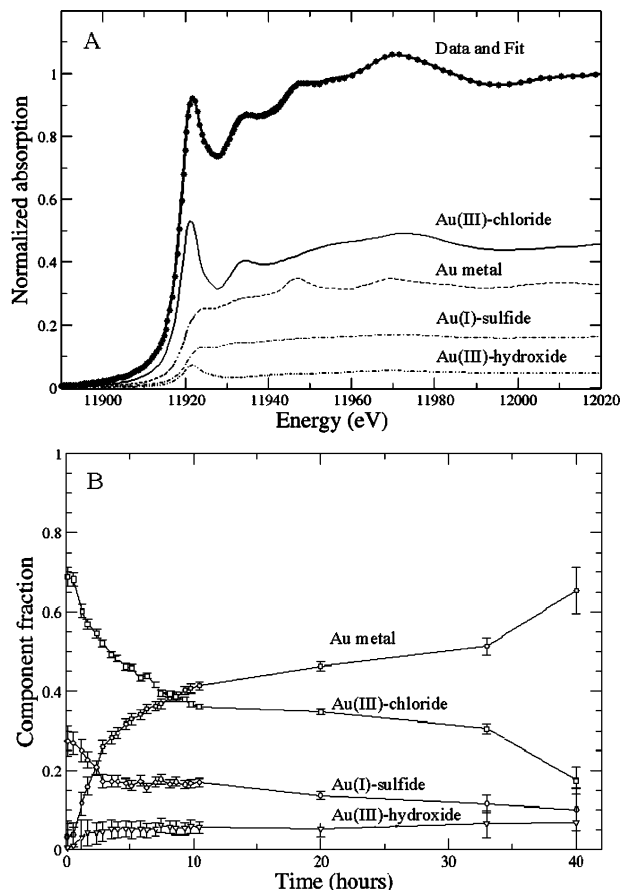


**FIGURE 3.** (A) XANES L<sub>3</sub>-edge spectrum and an example of an LC-XANES fit at 5 h and 12 min. The weighted components are displayed below the fit; (B) Inferred evolution of gold oxidation states and species with time at 7.6 mM initial gold in solution.

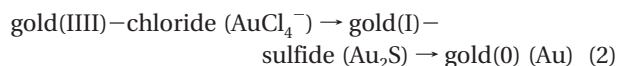
11947 and 11970 eV which are characteristic of Au(0), showed that Au(0) was not present in the samples.

At 7.6 mM initial gold, the spectra collected during the course of experiments showed significant change from the first to the last scans. Four model compounds including gold foil (Au), gold(III)–chloride, gold(I)–sulfide, and gold(III)–hydroxide showed the best match in the (linear combination) LC-XANES fits (Figure 3A). The results of the fits as a function of time are presented in Figure 3B. Gold(III)–chloride and gold(I)–sulfide decreased as gold(0) increased with time. The addition of a small amount of gold(III)–hydroxide consistently improved the fits. Because the gold(III)–hydroxide standard was prepared at a much higher pH than the cyanobacteria sample, we do not expect that it actually exists in this form in the sample. As in gold(III)–chloride solutions, the gold ion is stabilized in gold(III)–hydroxide solutions by a hydration shell. The addition of a small amount of the hydroxide standard in the LC-XANES fits thus compensates for the difference in pH between the gold(III)–chloride standard and the actual sample.

**EXAFS Spectra of the Cyanobacterial Samples.** The Fourier transforms, EXAFS spectra, and the results of fitting of the cyanobacteria sample at 0.8 mM initial gold are presented in the Supporting Information (Figure S5). Although there is evidence in the XANES spectra of the presence of gold foil, the EXAFS spectrum of the cyanobacteria sample is dominated by the signal of gold(I)–sulfide. A simultaneous fit was performed for the cyanobacteria sample along with the gold(I)–sulfide compound using a simple first shell fitting model. The results of the EXAFS fits are shown in the Supporting Information (Table S1). The Fourier transform range

for the gold(I)–sulfide model compound was  $2\text{--}11\text{ \AA}^{-1}$  and for the cyanobacterial sample  $2\text{--}10\text{ \AA}^{-1}$ , and the fitting range was from  $1.2\text{--}2.3\text{ \AA}$ . The level of noise in the cyanobacteria data precluded independent measurement of all the parameters listed above. Only by applying constraints between the cyanobacteria and gold(I)–sulfide data were we able to measure the parameters shown in the Supporting Information (Table S1). The sulfur coordination is diminished by almost a half of an atom in the presence of cyanobacteria relative to the aqueous gold(I)–sulfide standard. The Au–S bond length is nominally longer in the presence of cyanobacteria, but consistent with the standard with its error bar.

XAS has proven to be a powerful tool for investigating the speciation of various heavy metals in biomass (25–26). In this study, the XAS results showed that Au(III) was reduced to Au(I) in a very fast reaction (within minutes), and Au(I) was immediately coordinated with sulfur atoms from the cyanobacteria forming gold(I)–sulfide for all gold concentrations. Within the cyanobacteria, sulfur presumably was present as cysteine or methionine groups of the outer membrane or periplasmic proteins (27). This suggests that sulfur from cysteine or methionine groups of cyanobacteria was released to the bulk solutions through the outer membrane, and immediately bound with the reduced gold forming gold(I)–sulfide on the cells or at the cell walls (Figure 2). The cysteine or methionine within the outer membrane or periplasmic proteins also contained carbon and nitrogen, and this may explain the indirect relationship between nitrogen and gold (Supporting Information, Figure S2). As soft acids, gold(III) and gold(I) ions readily form complexes with nonpolar soft bases such as sulfur and nitrogen. Therefore, the interaction of a gold ion with sulfur would be expected. The reduction of Au(I) to Au(0) was a relatively slower process than the formation of gold(I)–sulfide, and was not observed by TEM until a reaction time of approximately 14 h for 0.8 mM and 1.7 mM initial gold, although XAS results indicated the precipitation of gold metal after 15 min (Figures 2 and 3). For the cyanobacteria sample at 7.6 mM initial gold, the reduction of Au(I) to Au(0) occurred after the addition of gold(III)–chloride to the cyanobacteria culture (Figure 3). Therefore, the steps for the mechanism of gold bioaccumulation by cyanobacteria are deduced to be as follows:



**Geochemical Implications for the Formation of Secondary Gold Deposits.** Gold concentrations in river and marine waters range up to about 50 ppb, while near gold deposits, soluble gold concentrations can be up to 1 ppm (28–29). Thus, the gold concentrations in natural environments are 2–3 orders of magnitude lower than those used in this study. This study showed that the gold reduction process from gold(III)–chloride to metallic gold by cyanobacteria was facilitated by higher gold concentrations. In natural environments where gold concentrations were relatively low, the reduction of gold(III)–chloride to metallic gold by cyanobacteria is presumably a slow process. In addition, at low gold concentrations (at ppb level), gold toxicity would not kill all viable bacterial cells; therefore, the remaining cells would be able to grow and probably adapt to the presence of gold (30).

The formation of an intermediate species, gold(I)–sulfide, shows the importance of organic reduced sulfur species in gold binding mechanisms by cyanobacteria. Passive gold accumulation via organic sulfur present in the cyanobacterial outer membrane or periplasma may explain the mechanisms of gold bioaccumulation by cyanobacteria. Organic sulfur species (e.g., cysteine, methionine) are present in other living microorganisms such as algae, plants, and fungi that could

be involved in the formation of secondary gold deposits. Also, the cycle of life through the decomposition of dying microorganisms in nature could lead to the formation of organic sulfur, for subsequent involvement in the precipitation of metallic gold.

The formation of metallic gold with octahedral habit has been observed by the interaction of gold(III)–chloride with cyanobacteria in this study as well as in natural environments from Mother Lode, California (31), weathered Archean metamorphic rocks in Western Australia (32), and the Witwatersrand gold deposit, South Africa (33–34). This study demonstrates that biogeochemical precipitation of metallic gold from gold(III)–chloride solutions could contribute to the formation of secondary gold in placer environments, and the importance of organic sulfur in the gold accumulation by cyanobacteria suggests the possible use of organic sulfur species as a biogeochemical indicator of the location of gold deposits.

**Application for Gold Recovery.** The recovery of gold from solutions has been actively studied for industrial purposes (16, 35–36). Mining, mineral processing, and metallurgical industries generate billions of tons of metal waste every year (37). Conventional methods for removing metals from ore processing solutions, including chemical precipitation, chemical oxidation or reduction, ion exchange, filtration, electrochemical treatment, membrane technologies, and evaporation, have been used for gold recovery (38). Because these processes are extremely expensive, alternative methods for metal recovery using living or dead microorganisms have been actively investigated (38).

This study shows that the cyanobacteria culture (*Plectononema boryanum* UTEX 485) was able to reduce Au(III) to Au(0) in solution; therefore, it can be used in biorecovery of gold from gold(III)–chloride solutions. In the present experiments, the cyanobacteria were killed by either the gold(III)–chloride reagent or the acidic pH and the resulting release of more organic sulfur caused further precipitation of gold (Figure 2). The interaction of the cyanobacteria (or organic materials from degradation of cyanobacteria) with gold(III)–chloride promoted the growth of metallic gold with (111) faces (18). The size of metallic gold particles with octahedral habit formed by the interaction of gold(III)–chloride with cyanobacteria increased with increasing gold concentrations from ~60 nm at 0.8 mM gold to 6  $\mu\text{m}$  at 7.6 mM gold within 24 h. These results indicate that the interaction of gold(III)–chloride with cyanobacteria can be used as a promising method for production of gold particles.

## Acknowledgments

We thank Dr. Steve Heald, Dr. Mahalingam Balasubramanian, Michael Pape, Dr. Marianna Krol, and Ronald Smith for their technical support. We also thank Dr. Janet G. Hering for handling this manuscript and two anonymous reviewers for their constructive comments. Experiments at the PNC/XOR facilities, Advanced Photon Source, Argonne National Laboratory, and research at these facilities were supported by the United States Department of Energy – Basic Energy Sciences, a major facilities access grant from the Natural Sciences and Engineering Research Council of Canada (NSERC), the University of Washington, Simon Fraser University, the Pacific Northwest National Laboratory, and the Advanced Photon Source. Use of the Advanced Photon Source was also supported by United States Department of Energy, Office of Science, Office of Basic Energy Sciences, under Contract No. W-31-109-Eng-38. Support for synchrotron efforts was also provided by the United States Department of Energy, Office of Science, Biological and Environmental Research, Environmental Remediation Science Program. The research at UWO was supported in part by the

## Supporting Information Available

Procedures for transmission electron microscopy (TEM) and X-ray absorption spectroscopy (XAS); results of the laboratory-based cyanobacterial experiments, TEM-EDS of a cyanobacterial cell in the presence of gold(III)–chloride solution, XANES spectra of the model compounds, and XAS spectra of the cyanobacterial samples. This material is available free of charge via the Internet at <http://pubs.acs.org>.

## Literature Cited

- Morteani, G. In *Gold: Progress in Chemistry, Biochemistry and Technology*; Schmidbaur, H., Ed.; Wiley and Sons, 1999; Chapter 2.
- Mann, A. W. Mobility of gold and silver in lateritic weathering profiles: Some observations from Western Australia. *Econ. Geol.* **1984**, *79*, 38–50.
- Webster, J. G. The solubility of gold and silver in the system Au–Ag–S–O<sub>2</sub>–H<sub>2</sub>O at 25 °C and 1 atm. *Geochim. Cosmochim. Acta.* **1986**, *50*, 1837–1845.
- Benedetti, M.; Boulegue, J. Mechanism of gold transfer and deposition in a supergene environment. *Geochim. Cosmochim. Acta.* **1991**, *55*, 1539–1547.
- Hallbauer, D. K. In *Mineral Deposits of South Africa*; Anhaeusser, C. R., Maske, S., Eds.; Geological Society of South Africa: Johannesburg, South Africa, 1986; Vols. I & II, pp 731–752.
- Watterson, J. R. Preliminary evidence for the involvement of budding bacteria in the origin of Alaska placer gold. *Geology* **1992**, *20*, 315–318.
- Bischoff, G. C. O.; Coenraads, R. R.; Lusk, J. Microbial accumulation of gold: an example from Venezuela. *N. Jb. Geol. Palaont. Abh.* **1992**, *185*, 131–159.
- Bischoff, G. C. O. Gold-adsorbing bacteria as colonizers on alluvial placer gold. *N. Jb. Geol. Palaont. Abh.* **1994**, *194*, 187–209.
- Bischoff, G. C. O. The biological origin of bacterioform gold from Australia. *N. Jb. Geol. Palaont. Mh.* **1997**, *H6*, 329–338.
- Mossman, D. J.; Reimer, T.; Durstling, H. Microbial processes in gold migration and deposition: modern analogues to ancient deposits. *Geosci. Can.* **1999**, *26*, 131–140.
- Dyer, B. D.; Krumbein, W. E.; Mossman, D. J. Nature and origin of stratiform kerogen seams in Lower Proterozoic Witwatersrand-type paleoplacers – the case for biogenicity. *Geomicrobiol.* **1994**, *12*, 91–98.
- Southam, G.; Beveridge, T. J. The in vitro formation of placer gold by bacteria. *Geochim. Cosmochim. Acta.* **1994**, *58*, 4527–4530.
- Southam, G.; Beveridge, T. J. The occurrence of bacterially derived sulfur and phosphorus within pseudocrystalline and crystalline octahedral gold formed in vitro. *Geochim. Cosmochim. Acta.* **1996**, *60*, 4369–4376.
- Kashefi, K.; Tor, J. M.; Nevin, K. P.; Lovley, D. R. Reductive precipitation of gold by dissimilatory Fe(III)-reducing bacteria and archaea. *Appl. Environ. Microbiol.* **2001**, *67*, 3275–3279.
- Nair, B.; Pradeep, T. Coalescence of nanoclusters and formation of submicron crystallites assisted by *Lactobacillus* strains. *Crystal Growth Des.* **2002**, *2*, 293–298.
- Nakajima, A. Accumulation of gold by microorganisms. *World J. Microbiol. Biotechnol.* **2003**, *19*, 369–374.
- Keim, C. N.; Farina, M. Gold and silver trapping by uncultured magnetotactic cocci. *Geomicrobiol. J.* **2005**, *22*, 55–63.
- Lengke, M. F.; Fleet, M. E.; Southam, G. Morphology of gold nanoparticles synthesized by filamentous cyanobacteria from gold(I)–thiosulfate and gold(III)–chloride complexes. *Langmuir* **2006**, *22*, 2780–2787.
- Tatrinov, A. V.; Yalovik, L. I.; Namsaraev, Z. B.; Plyusnin, A. N.; Konstantinova, K. K.; Zhmodik, S. M. Role of bacterial mats in the formation of rocks and ore minerals in travertines of nitric hydrothermal springs in the Baikal rift zones. *Dokl. Earth Sci.* **2005**, *403*, 939–943.
- Rippka, R.; Deruelles, J.; Waterbury, J.; Herdman, M.; Stanier, R. Y. Generic assignments, strain histories and properties of pure cultures of cyanobacteria. *J. Gen. Microbiol.* **1979**, *111*, 1–61.
- Nordstrom, D. K. Thermochemical redox equilibria of ZoBell's solution. *Geochim. Cosmochim. Acta.* **1977**, *41*, 1835–1841.
- Gardea-Torresdey, J. L.; Tiemann, K. J.; Gamez, G.; Dokken, K.; Cano-Aguilera, I.; Furenli, L. R.; Renner, M. W. XAS investigations into the mechanism(s) of Au(III) binding and reduction by alfalfa biomass. *Environ. Sci. Technol.* **2000**, *34*, 4392–4396.
- Pantelouris, A.; Kuper, G.; Holmes, J.; Feldmann, C.; Jansen, M. Anionic gold in Cs<sub>3</sub>AuO and Rb<sub>3</sub>AuO established by X-ray Absorption Spectroscopy. *J. Am. Chem. Soc.* **1995**, *117*, 11749–11753.
- Gammons, C. H.; Yu, Y.; Williams-Jones, A. E. The disproportionation of gold(I) chloride complexes at 25 to 200 °C. *Geochim. Cosmochim. Acta.* **1997**, *61*, 1971–1983.
- Kelly, R. A.; Andrews, J. C.; DeWitt, J. G. An X-ray absorption spectroscopic investigation of the nature of the zinc complex accumulated in *Datura innoxia* plant tissue culture. *Microchem. J.* **2002**, *71*, 231–245.
- Lopez, M. L.; Parson, J. G.; Vide, J. R. P.; Gardea-Torresdey, J. L. An XAS study of the binding and reduction of Au(III) by hop biomass. *Microchem. J.* **2005**, *81*, 50–56.
- Brock, T. D.; Madigan, M. T.; Martinko, J. M.; Parker, J. *Biology of Microorganisms*; Prentice Hall: Englewood Cliffs, NJ, 1994.
- Korobushkina, E. D.; Karavaiko, G. I.; Korobushkin, I. M. In *Environmental Biogeochemistry*; Hallberg, R., Ed.; Economic Bulletin: Stockholm, 1983; Vol. 35, pp 325–333.
- McHugh, J. B. Concentration of gold in natural waters. *J. Geochem. Explor.* **1988**, *30*, 85–94.
- Reith, F.; Rogers, S. L.; McPhail, D. C.; Webb, D. Biomineralization of gold: Biofilms on bacterioform gold. *Science* **2006**, *313*, 233–236.
- Leicht, W. California gold. *Min. Record* **1982**, *13* (7), 375–387.
- Wilson, A. F. Origin of quartz-free gold nuggets and supergene gold found in laterites and soils – a review and some new observations. *Aust. J. Earth Sci.* **1984**, *31*, 303–316.
- Frimmel, H. E.; LeRoex, A. P.; Knight, J.; Minter, W. E. A case study of the postdepositional alteration of the Witwatersrand Basal Reef Gold Placer. *Econ. Geol.* **1993**, *88*, 249–265.
- Minter, M. G.; Knight, J.; Frimmel, H. E. Morphology of Witwatersrand gold grains from the basal reef: evidence for their detrital origin. *Econ. Geol.* **1993**, *88*, 237–248.
- Pethkar, A. V.; Paknikar, K. M. Recovery of gold from solutions using *Cladosporium cladosporioides* biomass beads. *J. Biotechnol.* **1998**, *63*, 121–136.
- Romero-Gonzalez, M. E.; Williams, C. J.; Gardiner, P. H. E.; Gurman, S. J.; Habesh, S. Spectroscopic Studies of the Biosorption of Gold(III) by Dealginated Seaweed Waste. *Environ. Sci. Technol.* **2003**, *37*, 4163–4169.
- Eccles, H. Removal of heavy metals from effluent streams - why select a biological process? *Int. Biodeterior. Biodegrad.* **1995**, *35*, 5–16.
- Volesky, B. *Biosorption of Heavy Metals*; CRC Press Inc.: Boca Raton, FL, 1990.

Received for review May 1, 2006. Revised manuscript received July 29, 2006. Accepted July 31, 2006.

ES061040R